Received: 12 October 2020 | Accepted: 31 December 2020

DOI: 10.1111/1759-7714.13842

ORIGINAL ARTICLE

WILEY

HN1L promotes invasion and metastasis of the esophagogastric junction adenocarcinoma

Zhao Yang Wang[1] | Wen Xiao[1] | Yuan Zhu Jiang[1,2] | Wei Dong[1,2] | Xiang Wei Zhang[1,2] | Lin Zhang[1,2]

[1]Department of Thoracic Surgery, Shandong Provincial Hospital, Cheeloo College of Medicine, Shandong University, Jinan, Shandong, 250021, China

[2]Department of Thoracic Surgery, Shandong Provincial Hospital Affiliated to Shandong First Medical University, Jinan, Shandong, 250021, China

Correspondence
Lin Zhang, Department of Thoracic Surgery, Shandong Provincial Hospital, Cheeloo College of Medicine, Shandong University, 324th Jingwu Road, Jinan 250021, Shandong, China.
Email: doczhanglin@163.com

Funding information
Department of Science and Technology of Shandong Province, Grant/Award Number: 2016GSF201107; Jinan Science and Technology Development Program, Grant/Award Number: 201907112; Jinan Science and Technology Plan, Grant/Award Number: 201805070; National Natural Science Foundation of China, Grant/Award Number: 81802282

Abstract

Background: Adenocarcinoma of the esophagogastric junction (AEG) refers to cancer that crosses the line of the gastroesophageal junction and includes distal esophageal cancer and proximal gastric cancer. It is characterized by early metastasis and a poor prognosis and has few treatment options. Here, we report a novel potential therapeutic target, hematological and neurological expressed 1-like (*HN1L*), in AEG.

Methods: A total of 38 patients who underwent surgical resection of AEG at the Department of Thoracic Surgery of Shandong Provincial Hospital from September 2018 to June 2019 were enrolled into the study. We detected the expression of HN1L in AEG and adjacent nontumor tissues by IHC staining. The clinicopathological characteristics of *HN1L* were statistically analyzed. Then, the expression of *HN1L* in different cell lines was detected by RT-q PCR. Finally, AGS and HGC-27 cell lines were performed to inhibit *HN1L* by sh*RNA* in order to explore its role in the development of AEG.

Results: Immunohistochemical staining showed that the expression of HN1L in cancer tissues was higher than that in nontumor tissue ($p < 0.001$). High expression of HN1L was significantly correlated with TNM stage ($p = 0.013$) and lymph node metastasis ($p = 0.03$). The expression of *HN1L* was upregulated in tumor cell lines compared with normal cell line. Additionally, Cell function studies demonstrated that lentivirus-mediated sh*RNA* silencing of *HN1L* expression could effectively reduce the proliferation, invasion, and metastasis of tumor cell lines and promote their apoptosis ($p < 0.05$).

Conclusions: *HN1L* expression might contribute to the invasion and metastasis of AEG and is a promising therapeutic target.

KEYWORDS
adenocarcinoma of the esophagogastric junction, HN1L, invasion, metastasis, proliferation

INTRODUCTION

In the past two decades, the incidence rate of adenocarcinoma of the esophagogastric junction (AEG) has rapidly increased.[1] Because of the lack of early symptoms, AEG patients often have extensive locoregional invasion and distant metastasis at the time of first diagnosis. Furthermore, there are no targeted therapies, and thus the prognosis is poor.[2,3] Although great progress has been made in surgery and chemoradiotherapy, the overall five-year survival rate remains at 10%–15%.[2] Tumor development is a multistep process that involves many genes and proteins.[4] Investigation of the roles of various oncogenes in the abnormal proliferation of AEG is of great significance for revealing the tumorigenic mechanism of AEG and identifying new therapeutic targets.

Human hematological and neurological expressed 1-like (*HN1L*) was first identified in a mouse fertilized egg cDNA library in 2000.[5] It belongs to the hematological and neurological expressed 1 (*HN1*) family.[6] *HN1* and *HN1L* are

Zhao Yang Wang and Wen Xiao made the same contribution to the article.

This is an open access article under the terms of the Creative Commons Attribution-NonCommercial-NoDerivs License, which permits use and distribution in any medium, provided the original work is properly cited, the use is non-commercial and no modifications or adaptations are made.
© 2021 The Authors. *Thoracic Cancer* published by China Lung Oncology Group and John Wiley & Sons Australia, Ltd

widely expressed in many tissues during the embryonic development of rodents, including nerve tissue and immature retina.[7,8] Knockdown of *HN1* by siRNA in a murine melanoma cell line, B16-F10, could promote cell differentiation and induce cell cycle arrest.[8] This indicates that *HN1* has an important role in the regulation of the cell cycle. Additionally, HN1 promotes prostate cell migration by controlling the stability of the interaction between β-catenin and E-cadherin in adhesion junctions.[9] In addition, *HN1* silencing could significantly slow down tumor growth after intracerebral xenotransplantation of murine GL261 glioma cells.[10] It has also been shown to be overexpressed in breast[11] and pancreatic cancer[12] and is significantly associated with poorer overall survival in these cancer patients. This evidence suggests that *HN1* has an important role in regulating the proliferation and metastasis of cancer cells. *HN1L* is located on chromosome 16p13.3 and encodes a 190-amino acid protein. HN1L protein is mainly located in the cytoplasm, and is specifically expressed in many human tissues, such as the liver, lung, breast, testis, and uterus.

Previous studies have found that overexpression of HN1L can promote the malignant proliferation of lung cancer cells by activating the MAPK pathway.[13] In addition, it has a similar effect on breast cancer cells through the LEPR–STAT3 pathway.[14] The invasion of hepatocellular carcinoma is also promoted by the HN1L–AP-2γ–METTL13–TCF3–ZEB1 pathway.[15] Ultimately, it has a negative impact on the overall survival of these cancer patients. However, its exact role in AEG has not been determined. This study investigated the expression levels of HN1L in AEG and its adjacent nontumor tissues, and further explored the correlation between HN1L expression and clinical parameters and its prognostic value. We confirmed the regulatory effect of the *HN1L* gene on the malignant proliferation of human gastric cancer cell lines. In this study, we found that knockdown of *HN1L* could effectively inhibit tumor growth, invasion, and metastasis which indicates that *HN1L* expression may have an important role in the development of AEG.

TABLE 1 Clinicopathological characteristics related to HN1L expression in AEG

Parameters	Case	Level of *HN1L* expression		*p*-value
		>median values (n)	<median values (n)	
Sex				0.709
Male	28	16	12	
Female	10	7	3	
Age (years)				0.728
<60	12	8	4	
≥60	26	15	11	
Tumor size (cm)				1.000
≤5	24	15	9	
>5	14	8	6	
pTNM stage				0.013
Stage I II	13	4	9	
Stage III IV	25	19	6	
Depth of invasion				0.223
T1–T2	8	3	5	
T3–T4	30	20	10	
Lymph node metastasis				0.030
Positive	28	20	8	
Negative	10	3	7	
Grade of differentiation				0.509
1/1–2/2	17	9	8	
2–3/3	21	14	7	
Survival				0.138
Yes	34	19	15	
No	4	4	0	
Siwert style				0.440
I	8	6	2	
II	30	17	13	

METHODS

Patients and tissue samples

A total of 38 patients who underwent surgical resection of adenocarcinoma of the esophagogastric junction (AEG) at the Department of Thoracic Surgery of Shandong Provincial Hospital from September 2018 to June 2019 were enrolled. All patients (Siewert AEG types I and II) were treated by Ivor Lewis minimal invasive esophagectomy (MIE) with systematic D2-lymphadenectomy and did not receive neoadjuvant chemotherapy prior to surgery. The tumor samples and matched normal samples were all from tissues excised during surgery and the postoperative pathological results showed that the cut edges were negative. The pTNM staging of all patients was performed according to the American Joint Committee on Cancer (AJCC) eighth edition. Medical records and follow-up data were obtained from telephone follow-up and patients' medical records. This project was approved by the ethical committee of Shandong Provincial Hospital. The clinicopathological characteristics of the patients are summarized in Table 1.

Immunohistochemistry

All specimens were fixed in 10% neutral formalin, embedded in paraffin blocks, and cut into sections (5 μm thick). Primary HN1L antibody was diluted 1:100 (ab200587; Abcam). UltraSensitive SP (Mouse/Rabbit) IHC Kit (KIT-9720; Maixin) was used as the secondary antibody for visualization. Immunoperoxidase was detected using the Vulcan Fast Red Chromogen Kit 2 (Linaris) and diaminobenzidine substrate. The preparations were slightly stained with hematoxylin, fixed with resin, and examined with a light microscope. The staining was scored using the intensity of the positive staining (0, negative; 1, weak; 2, moderate; and 3, strong) multiplied by the stained areas (0, negative;

1, 1%–25%; 2, 25%–50%; 3, 50%–75%; and 4, 75%–100%). Two scores were multiplied as the final score (negative, 0; weak, 1–3; moderate, 4–9; and strong, 10–12). These scores were independently determined by two pathologists.

Cell lines and cell culture

In the sixth edition of the American Joint Commission on Cancer (AJCC6) staging system, cardiac cancer involving the esophagus is traditionally considered to be gastric cancer.[16] There is also no specific AEG cell line that has been cultured, and gastric cancer (GC) cell lines were therefore selected as an alternative experimental model, taking into consideration the similarity of pathological types.[17,18] In this set of experiments, four human GC cell lines, AGS (ATCC CRL-1739; USA), MKN-45 (KeyGEN), HGC-27 (Cell Bank of the Chinese Academy of Sciences), and MGC80-3 (Genechem) were selected as the candidate lines for cytological tests, Human normal gastric epithelial cell line GES-1 (KeyGEN) as negative control. MKN-45, HGC-27, MGC80-3 and GES-1 cells were cultured in RPMI-1640 medium. AGS cells were cultured in F12K medium (Sigma). All media were supplemented with 10% fetal bovine serum. Cells were maintained at 37°C with 5% CO_2. The mRNA expression of *HN1L* in different cell lines was detected by RT-qPCR. According to their expression levels, two cell lines were selected for cell function tests after incubation at 37°C in 5% CO_2 for 72 h. The targeted *HN1L* sequence was (sense sequence): 5′-CTAATAGGATGGCATCTAA -3′.

RNA extraction and RT-q PCR

RNA isolation and RT-qPCR were performed according to the manufacturer's instructions. Trizol reagents (Pufei) were utilized for total RNA extraction. Total RNA was reverse-transcribed to cDNA using a M-MLV RTase kit (Promega). RT-qPCR was performed to detect gene expression with SYBR Premix Ex Taq (Takara). Primers targeting *HN1L* and *GAPDH* were obtained from RiboBio. *GAPDH* was used as an endogenous control for *HN1L*. The expression of *HN1L* in different cell lines was evaluated by ΔCt. And the subsequent gene knockdown efficiency of *HN1L* compared with the control group was reflected by $2^{-\Delta\Delta Ct}$. The primers were as follows: *HN1L* (F: 5′- CTTGGCACACCCAAACAAACC-3′; R:5′-CCTTGCAGCTTTAAGATCCGATT−3′); and *GAPDH* (F:5′-TGACTTCAACAGCGACACCCA-3′; R:5′-CACCCTG TTGCTGTAGCCAAA-3′).

Lentivirus shRNA, plasmids, and transfection

shRNA interference sequence targeting *HN1L* was designed and synthesized by Generay using human HN1L cDNA GenBank accession no. NM_144570. The sense sequence of *HN1L* shRNA-1 was as follows: 5′-CCGGGCCTAATAGG ATGGCATCTAACTCGAGTTAGATGCCATCCTATTAG-GCTTTTTG-3′; and shRNA-2: 5′-AATTCAAAAAGCC TAATAGGATGGCATCTAACTCGAGTTAGATGCCATC CTATTAGGC-3′. The negative control sequence was: 5′-TTCTCCGAACGTGTCACGT-3′. The dsDNA oligo product was cloned into GV115 vector (Genechem) using *AgeI* and *EcoRI* restriction enzymes and then the recombinant plasmid GV115 product was transformed into competent *E. coli* cells (cat. #CB104-03; Tiangen). The positive transformants were identified by PCR and sequencing. PCR conditions were as follows: 94°C for 3 min, followed by 22 cycles of 94°C for 30 s, 55°C for 30 s, and 72°C for 30 s, and then 72°C for 5 min. The plasmid was extracted according to the instructions of the EndoFree Maxi Plasmid Kit (cat. no. DP117; Tiangen). The previously selected cell lines were transfected with positive GV115 vector and *HN1L* knockdown efficiency was confirmed by RT-qPCR and western blotting.

Western blotting

Cells were washed twice with PBS buffer and lysed in RIPA lysis buffer on ice. Equivalent quantities of total protein (35 μg) were resolved by 12% sodium dodecyl sulfate-polyacrylamide gel electrophoresis (SDS-PAGE) and detected by western blotting using anti-HN1L (1:5000; ab200587; Abcam) and anti-GAPDH (1:2000; sc-32233) antibodies. After hybridization of secondary antibodies, proteins were detected using an enhanced chemiluminescence (ECL) detection kit (M32106; Thermo) in accordance with the manufacturer's recommendations.

Celigo cell proliferation assay

The experimental and control cells were seeded into 96 well-plates at a density of 2000 cells/well and cultured at 37°C with 5% CO_2. Cells were counted by a Celigo Imaging Cytometer (Nexcelom Bioscience) every day, and a cell proliferation curve was drawn after five consecutive days of counting.

Colony formation assay

A total of 1×10^3 cancer cells were seeded into a six-well plate with soft agar mixture as medium for eight days. The surviving colonies (>50 cells) were counted after staining with crystal violet (Sangon Biotech). Colony forming ability was used to evaluate cell proliferation and independent survival. Triplicate independent experiments were performed.

Apoptosis assay

Cells were seeded into six-well plates (5×10^5 cells/well) and apoptosis was analyzed by staining with Annexin V-APC (eBioscience) according to the manufacturer's

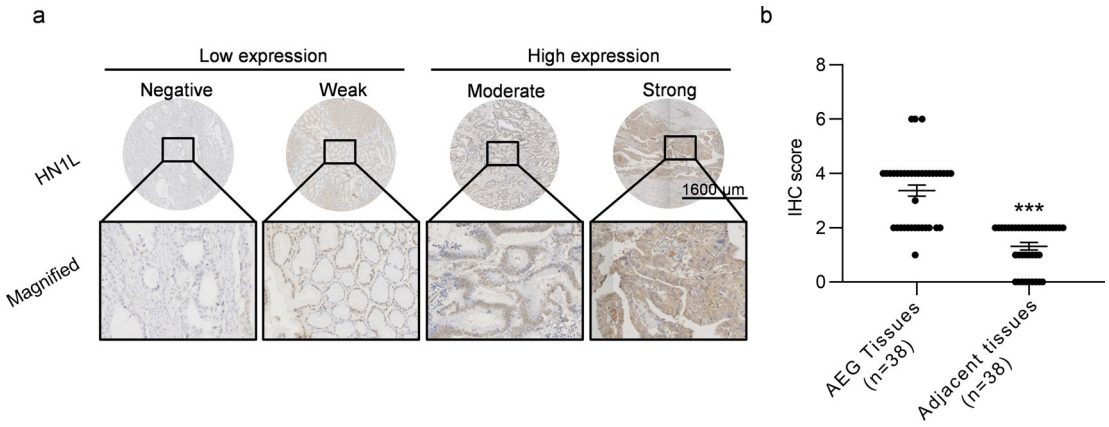

FIGURE 1 *HN1L* was highly expressed in AEG. (a) Representative IHC staining images with different scores were calculated according to the intensity and percentage of stained AEG cells. Magnification ×200; scale bar, 1600 μm. (b) Quantification of *HN1L* expression according to IHC scores in 38 AEG tissues and corresponding adjacent nontumor tissues. AEG, adenocarcinoma of the esophagogastric junction; IHC, immunohistochemistry. Data are shown as mean ± SD. ***$p < 0.001$, based on Student's *t*-test

instructions. The proportion of apoptotic cells was detected by flow cytometry (BD).

MTT assay

Before use, cells transfected with sh*Ctrl* and sh*HN1L* were plated into 96-well plates at a concentration of 2×10^3 cells/well. On days 1, 2, 3, 4, and 5, 20 μl MTT (5 mg/ml) was added to each well. After further incubation for 4 h, 100 μl DMSO was added to each well. After shaking at low speed for 5 min, the optical density of each well at 490 nm (OD490) was measured by a microplate reader (M2009PR, Tecan infinite), and cell proliferation curves were drawn.

Cell migration and invasion assays

Migration and invasion experiments were performed by transwell assay. For migration assays, transfected cells were seeded at a density of 1×10^5 cells in 24-well transwell chambers with 8-μm polycarbonate membrane (Corning, New York, USA), and 100 μl serum-free medium was added to the upper chamber. Next, 600 μl medium containing 30% fetal bovine serum was added to the lower chamber and the cells were cultured at 37°C for 18 h for migration. After the cells on the upper surface of the filter were removed with cotton swabs, the migrating cells attached to the lower surface of the membrane were fixed with 4% paraformaldehyde solution, stained with 0.5% crystal violet, and counted in nine random fields under the microscope. For invasion assays, a Matrigel coating was added to the polycarbonate membrane. Three independent experiments were performed.

Statistical analysis

All statistical analyses were performed using STATA software version 15.1 (STATA, College Station, TX, USA). Paired student's *t*-test was used to compare the expression levels of *HN1L* between tumor and adjacent tissues. Fisher's exact test was used to analyze the correlation between HN1L IHC score and clinicopathological features. In all statistical analyses, $p < 0.05$ was considered statistically significant.

RESULTS

Associations between HN1L and clinicopathological variables

We first detected the expression of HN1L in 38 patients with primary AEG by IHC. As shown in Figure 1, HN1L was mainly located in the cytoplasm of tumor cells. We observed that HN1L was expressed in almost all human AEG tissues and many normal tissues. The protein levels in tumor tissues were significantly higher than those in normal tissues ($p < 0.001$) (Figure 1(b)). In this study, the IHC staining score of HN1L in tumor tissue was used to evaluate its expression level and was 1–6 with a mean of 3.4. Patients were divided into a low expression group and a high expression group according to whether HN1L levels were higher or lower than the mean. The relationship between HN1L expression and clinicopathological features is summarized in Table 1. The expression of HN1L was significantly correlated with TNM stage ($p = 0.013$) and lymph node metastasis ($p = 0.03$). However, there was no significant correlation with sex, age, tumor size, depth of invasion, differentiation level, and Siewert classification. The follow-up period of all 38 patients ranged from 5 to 22 months, with an average of 17.2 months. The overall survival rate in the high expression group and low expression group was 82.6 and 100%, respectively, and the progression-free survival rate was 73.9 and 80%. We noticed that during the follow-up

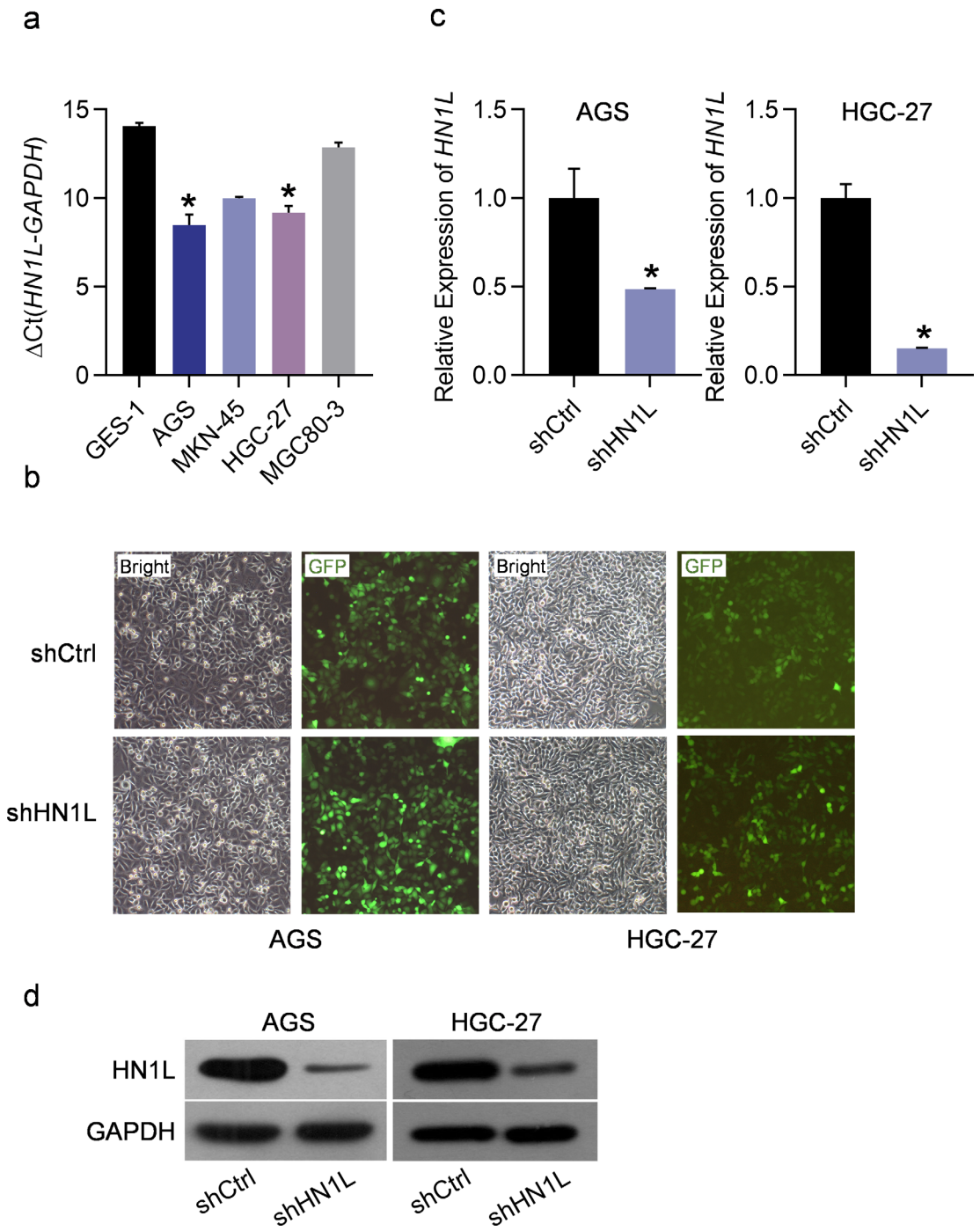

FIGURE 2 Construction of lentivirus and detection of knockdown efficiency. (a) RT-qPCR was used to detect the expression of *HN1L* relative to *GAPDH* in GES-1 cell line and four GC cell lines. (b) Morphology and fluorescence images of AGS and HGC-27 cells transfected with sh*Ctrl* and sh*HN1L* lentivirus. Magnification, ×100. (c) RT-qPCR assay showed that the expression levels of *HN1L* in AGS and HGC-27 cells were significantly lower than those in the control group after *HN1L* knockdown ($p < 0.05$). The total knockdown efficiency was more than 50%. (d) Protein expression levels of HN1L analyzed by western blotting in AGS and HGC-27 cells. Data are representative of three independent experiments and are shown as mean ± SD. *$p < 0.05$, based on Student's *t*-test

period, all deaths were in the high HN1L expression group. Because of the limitations of the sample size and follow-up time, there was no significant difference in overall mortality between the two groups. Nonetheless, it is a reasonable suspicion that high expression of *HN1L* may be associated with the poor prognosis of AEG patients.

To determine the role of *HN1L* in AEG cancer, *HN1L* expression was first examined in several human GC cell lines as well as GES-1, a normal epithelial cell line. As shown

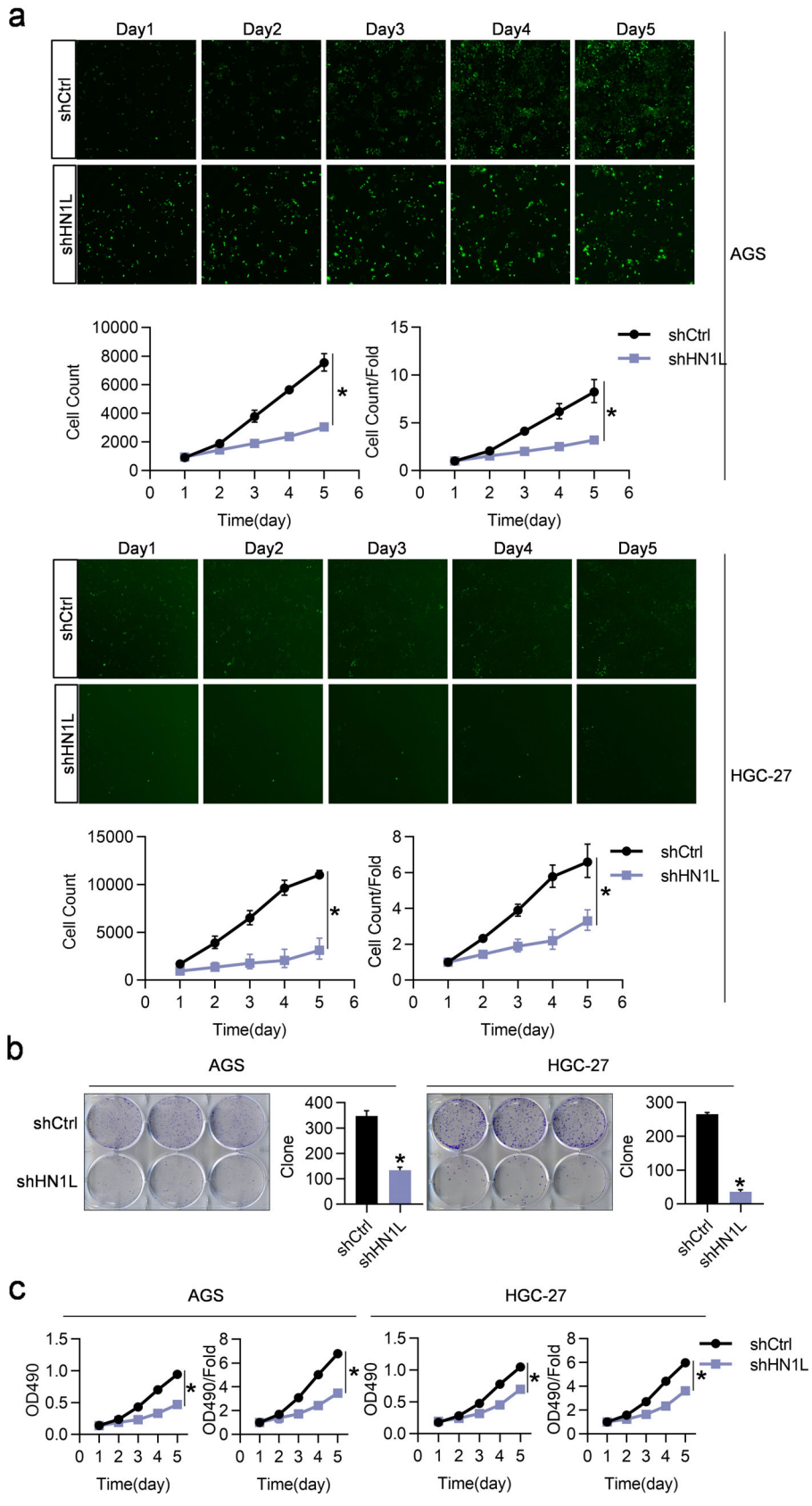

FIGURE 3 *HN1L* knockdown inhibited tumor proliferation in vitro. (a) Fluorescence images of cells were analyzed by Celigo high-content screening assay. The upper panel is the representative image, and the lower panel is the growth curve. Magnification, ×100 ($p < 0.05$). (b) In colony formation assays of AGS and HGC-27 cells, colonies containing more than 50 cells were counted and plotted ($p < 0.05$). (c) MTT cell proliferation assay showed that sh*HN1L* significantly inhibited the proliferation of AGS and HGC-27 cells ($p < 0.05$). Data are representative of three independent experiments and are shown as mean ± SD. *$p < 0.05$, based on Student's *t*-test

in Figure 2(a), the expression of *HN1L* was upregulated in AGS, MKN-45, HGC-27, MGC80-3 cells compared with GES-1 cell line, and *HN1L* mRNA levels in AGS and HGC-27 cells were higher than other human GC cell lines. Therefore, we chose AGS and HGC-27 cells for *HN1L* knockdown experiments.

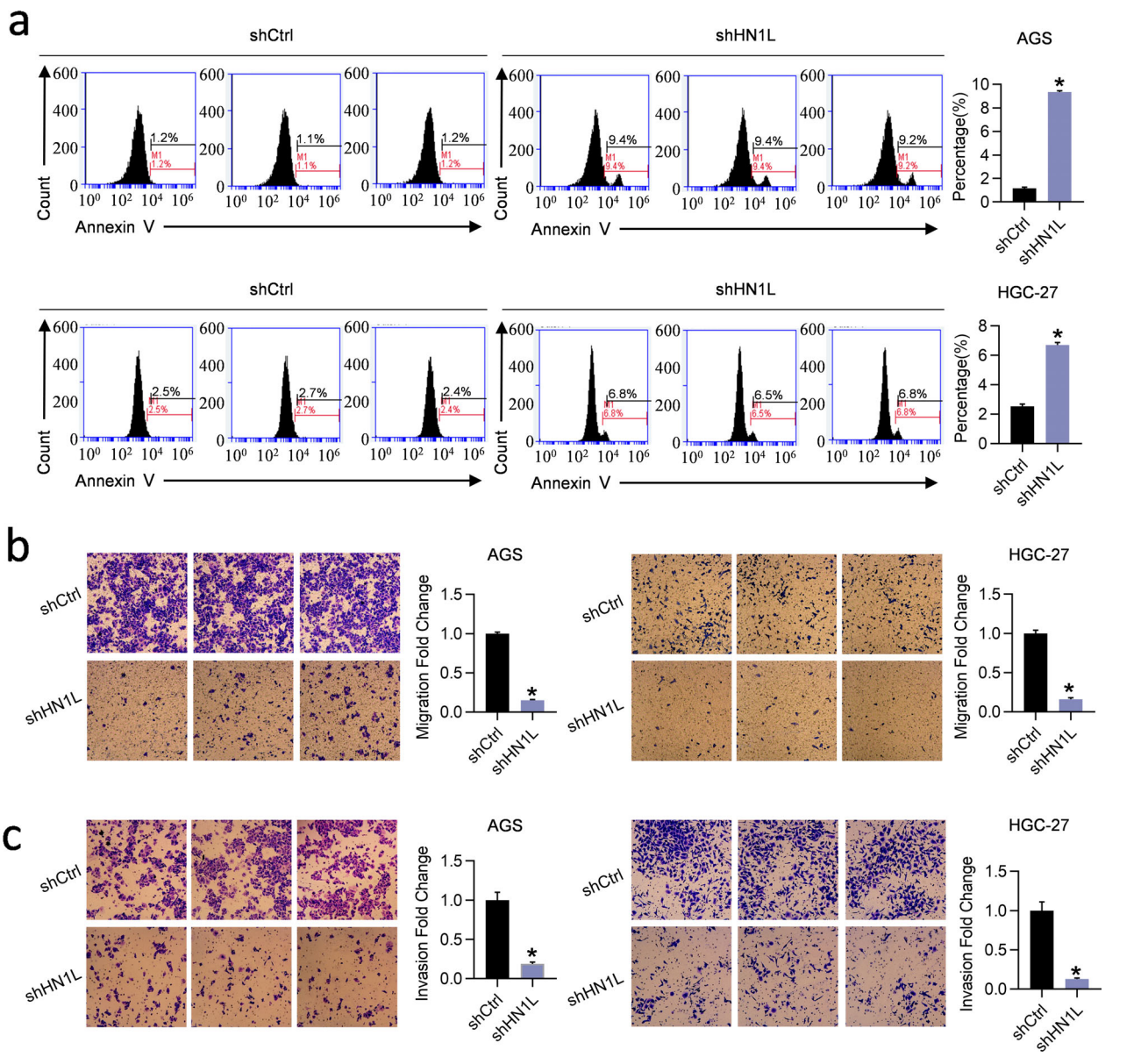

FIGURE 4 *HN1L* knockdown inhibited tumor invasion and metastasis and promoted apoptosis in vitro. (a) Apoptotic rate of AGS and HGC-27 cells transfected with sh*Ctrl* or sh*HN1L*. The apoptotic rate of the sh*HN1L* group was significantly higher than that of the sh*Ctrl* group ($p < 0.05$). (b) The effect of stable *HN1L* knockdown on the migration ability of AGS and HGC-27 cells was detected by transwell migration assay ($p < 0.05$). (c) Invasion ability was detected by transwell Matrigel invasion assay ($p < 0.05$). Magnification, ×200. Data are representative of three independent experiments and are shown as mean ± SD. *$p < 0.05$

Knockdown of HN1L inhibited AEG cell proliferation in vitro

To further study the role of *HN1L* in AEG, we constructed expression vectors GV115-NC and GV115-sh*HN1L* and used lentivirus-mediated shRNA to knockdown *HN1L* in AGS and HGC-27 cell lines. As shown in Figure 2(b), the percentage of infected cells in the sh*Ctrl* and sh*HN1L* groups reached over 80%. *HN1L* expression in the sh*HN1L* group was significantly decreased compared with the sh*Ctrl* group in AGS and HGC cells, as detected by RT-qPCR (Figure 2(c)) ($p < 0.05$) and western blotting (Figure 2(d)). To study the effect of *HN1L* on cell proliferation, MTT and Celigo assays were performed to detect cell proliferation for 5 days. As shown in Figure 3(a) and (c), *HN1L* knockdown significantly inhibited cell proliferation. Colony formation assays also showed similar results ($p < 0.05$) (Figure 3(b)), which suggests that *HN1L* is significantly related to the proliferation of AEG cells in vitro.

Knockdown of HN1L increased cell apoptosis

We used flow cytometry to determine whether *HN1L* expression is associated with apoptosis. The results showed that in AGS and HGC-27 cell lines, the percentage of

apoptotic cells in the sh*HN1L* group was significantly higher than that in the sh*Ctrl* group (average from AGS, 1.16%–9.34%; HGC-27, 2.55%–6.69%) ($p < 0.05$) (Figure 4(a)). These results suggest that *HN1L* knockdown could promote the apoptosis of AEG cells.

Knockdown of HN1L enhances cell invasion and migration

Transwell migration assays showed that *HN1L* knockdown significantly inhibited the migration of AGS and HGC-27 cell lines (Figure 4(b)) ($p < 0.05$). Similar to the migration assays, Matrigel cell invasion assays also showed significant differences between the sh*Ctrl* and sh*HN1L* groups (Figure 4 (c)) ($p < 0.05$). Therefore, these in vitro studies indicated that *HN1L* is significantly related to the migration and invasion of AEG cells.

DISCUSSION

The incidence of AEG is higher than that of distal gastric cancer.[1] Moreover, it differs from distal gastric cancer in terms of age, sex, incidence rate, tumor biological behavior, and clinicopathological characteristics.[19] Therefore, we investigated AEG as an independent tumor type. In this study, the expression of *HN1L* in 38 AEG specimens was detected by IHC staining and compared with that in normal mucosa. IHC staining showed that high HN1L expression was positively correlated with tumor pTNM stage and lymph node metastasis. To ensure the homogeneity of the enrolled patients, we excluded many patients who received preoperative neoadjuvant chemotherapy or who underwent left thoracic approach surgery. This limited the sample size and follow-up time. Therefore, we did not analyze the relationship between *HN1L* expression and survival. But, pTNM staging is significantly related to the prognosis of AEG patients as a general consensus and has been confirmed in many articles.[20,21] Therefore, we can reasonably infer that high expression of *HN1L* is related to the poor prognosis of AEG patients. Extended follow-up results and expanded sample sizes will be obtained in subsequent studies to further verify the relationship between *HN1L* expression and the prognosis of AEG patients.

Zhou et al.[6] completed the cloning and identification of human *HN1L* as early as 2004. However, the physiological function of *HN1L* in humans remains unclear.[22] At present, there are limited articles on the correlation between *HN1L* and different tumor types. Published studies on the correlation between *HN1L* and the occurrence and development of breast, liver, and non-small cell lung cancer differ regarding the mechanism of gene effects on cell phenotype.[13–15] In this study, we discussed the carcinogenic role of *HN1L* in the progression of AEG. According to the information in the Gene Expression Profiling Interactive Analysis (GEPIA) database, *HN1L* is expressed differentially between tumor and normal tissues in many different cancer types, but its expression in AEG is not described separately. The difference in *HN1L* expression in gastric cancer cells in the GEPIA database was consistent with our IHC results in AEG cells. We ultimately selected gastric cancer cell lines (AGS and HGC-27) as the cytological test models, which can be widely observed in many studies on AEG.[17,18,23] *HN1L* was knocked down in AGS and HGC-27 cell lines in vitro. The results showed that *HN1L* knockdown significantly reduced the proliferative ability of AGS and HGC-27 cells and induced their apoptosis. It is also effective in inhibiting cell migration and invasion. These results suggest that HN1L is a potential therapeutic target in AEG patients.

Research on potential targets of AEG cells has been of great focus. Sun et al.[24] considered that transcriptional coactivator with PDZ-binding motif (TAZ)- and β-catenin-targeted therapy for AEG is a promising treatment. Li et al.[25] considered that p21 protein (Cdc42/Rac)-activated kinase 1 (PAK1) is an important node in the PAK1–HER2–EGFR network, and may also be a potential target molecule. The mesenchymal–epithelial transition factor (MET) gene is also a hot point for AEG-targeted therapy.[26,27] However, there are still no effective first-line targeted drugs for AEG in clinical practice. At present, targeted therapies with a known survival benefit in AEG are limited to trastuzumab for HER2-overexpressing cancers or ramucirumab for VEGFR-2.[28,29] Even for gastric cancer, there are still very few targeted drugs.[30] Although our study suggests that HN1L can be used as a potential therapeutic target for AEG, whether HN1L can really benefit clinical treatment requires further research in gene-related protein pathways and animal experiments prior to phase III clinical trials to clarify these data. Further exploration of these pathways is in progress, and lentivirus-mediated shRNA combined with chemoradiotherapy may be a potential treatment approach for AEG.

In conclusion, we demonstrated high expression of HN1L in AEG cells by IHC. Inhibition of *HN1L* by lentivirus reduces the proliferation, invasion, and migration of tumor cells and promotes their apoptosis. To our knowledge, this is the first study on the significance of HN1L expression in AEG. It provides a new reference point for targeted therapy and prognosis evaluation for AEG. Further studies are required to confirm the clinical significance of HN1L as a therapeutic target.

ACKNOWLEDGMENTS

This study was supported by the Department of Science and Technology of Shandong Province (No.2016GSF201107), National Natural Science Foundation of China (81802282), Jinan Science and Technology Plan (201805070), and Jinan Science and Technology Development Program (201907112).

CONFLICT OF INTEREST

No authors report any conflict of interest.

REFERENCES

1. Hasegawa S, Yoshikawa T. Adenocarcinoma of the esophagogastric junction: incidence, characteristics, and treatment strategies. Gastric Cancer. 2010;13(2):63–73.
2. Feith M, Stein HJ, Siewert JR. Adenocarcinoma of the esophagogastric junction: surgical therapy based on 1602 consecutive resected patients. Surg Oncol Clin N Am. 2006;15(4):751–64.
3. Siewert JR, Stein HJ, Feith M. Adenocarcinoma of the esophagogastric junction. Scand J Surg. 2006;95(4):260–9.
4. Gu ZD, Li JY, Li M, Gu J, Shi XT, Ke Y, et al. Matrix metalloproteinases expression correlates with survival in patients with esophageal squamous cell carcinoma. Am J Gastroenterol. 2005;100(8):1835–43.
5. Ko MS, Kitchen JR, Wang X, Threat TA, Wang X, Hasegawa A, et al. Large-scale cDNA analysis reveals phased gene expression patterns during preimplantation mouse development. Development. 2000;127 (8):1737–49.
6. Zhou G, Wang J, Zhang Y, Zhong C, Ni J, Wang L, et al. Cloning, expression and subcellular localization of HN1 and HN1L genes, as well as characterization of their orthologs, defining an evolutionarily conserved gene family. Gene. 2004;331:115–23.
7. Goto T, Hisatomi O, Kotoura M, Tokunaga F. Induced expression of hematopoietic- and neurologic-expressed sequence 1 in retinal pigment epithelial cells during newt retina regeneration. Exp Eye Res. 2006;83(4):972–80.
8. Laughlin KM, Luo D, Liu C, Shaw G, Warrington KH Jr, Law BK, et al. Hematopoietic- and neurologic-expressed sequence 1 (Hn1) depletion in B16.F10 melanoma cells promotes a differentiated phenotype that includes increased melanogenesis and cell cycle arrest. Differentiation. 2009;78(1):35–44.
9. Varisli L, Ozturk BE, Akyuz GK, Korkmaz KS. HN1 negatively influences the β-catenin/E-cadherin interaction, and contributes to migration in prostate cells. J Cell Biochem. 2015;116(1):170–8.
10. Laughlin KM, Luo D, Liu C, Shaw G, Warrington KH Jr, Qiu J, et al. Hematopoietic- and neurologic-expressed sequence 1 expression in the murine GL261 and high-grade human gliomas. Pathol Oncol Res. 2009;15(3):437–44.
11. Zhang ZG, Chen WX, Wu YH, Liang HF, Zhang BX. MiR-132 prohibits proliferation, invasion, migration, and metastasis in breast cancer by targeting HN1. Biochem Biophys Res Commun. 2014;454(1): 109–14.
12. Zhang C, Xu B, Lu S, Zhao Y, Liu P. HN1 contributes to migration, invasion, and tumorigenesis of breast cancer by enhancing MYC activity. Mol Cancer. 2017;16(1):90.
13. Li L, Zeng TT, Zhang BZ, Li Y, Zhu YH, Guan XY. Overexpression of HN1L promotes cell malignant proliferation in non-small cell lung cancer. Cancer Biol Ther. 2017;18(11):904–15.
14. Liu Y, Choi DS, Sheng J, Ensor JE, Liang DH, Rodriguez-Aguayo C, et al. HN1L promotes triple-negative breast cancer stem cells through LEPR-STAT3 pathway. Stem Cell Rep. 2018;10(1):212–27.
15. Li L, Zheng YL, Jiang C, Fang S, Zeng TT, Zhu YH, et al. HN1L-mediated transcriptional axis AP-2γ/METTL13/TCF3-ZEB1 drives tumor growth and metastasis in hepatocellular carcinoma. Cell Death Differ. 2019;26(11):2268–83.
16. Huang Q, Shi J, Feng A, Fan X, Zhang L, Mashimo H, et al. Gastric cardiac carcinomas involving the esophagus are more adequately staged as gastric cancers by the 7th edition of the American Joint Commission on Cancer Staging System. Mod Pathol. 2011;24(1):138–46.
17. Matula K, Collie-Duguid E, Murray G, Parikh K, Grabsch H, Tan P, et al. Regulation of cellular sphingosine-1-phosphate by sphingosine kinase 1 and sphingosine-1-phopshate lyase determines chemotherapy resistance in gastroesophageal cancer. BMC Cancer. 2015;15:762.
18. Schimanski CC, Jordan M, Schlaegel F, Schmidtmann I, Lang H, Galle PR, et al. SNP rs1801157 significantly correlates with distant metastasis in CXCL12 expressing esophagogastric cancer. Int J Oncol. 2011;39(2):515–20.
19. Shan L, Ying J, Lu N. HER2 expression and relevant clinicopathological features in gastric and gastroesophageal junction adenocarcinoma in a Chinese population. Diagn Pathol. 2013;8:76.
20. Amin MB, Greene FL, Edge SB, Compton CC, Gershenwald JE, Brookland RK, et al. The eighth edition AJCC cancer staging manual: continuing to build a bridge from a population-based to a more "personalized" approach to cancer staging. CA Cancer J Clin. 2017;67(2):93–9.
21. Liu K, Feng F, Chen XZ, Zhou XY, Zhang JY, Chen XL, et al. Comparison between gastric and esophageal classification system among adenocarcinomas of esophagogastric junction according to AJCC 8th edition: a retrospective observational study from two high-volume institutions in China. Gastric Cancer. 2019;22(3):506–17.
22. Mitchell A, Chang HY, Daugherty L, Fraser M, Hunter S, Lopez R, et al. The InterPro protein families database: the classification resource after 15 years. Nucleic Acids Res. 2015;43(Database issue):D213–21.
23. Watanabe N, Komatsu S, Ichikawa D, Miyamae M, Ohashi T, Okajima W, et al. Overexpression of YWHAZ as an independent prognostic factor in adenocarcinoma of the esophago-gastric junction. Am J Cancer Res. 2016;6(11):2729–36.
24. Sun L, Chen F, Shi W, Qi L, Zhao Z, Zhang J. Prognostic impact of TAZ and β-catenin expression in adenocarcinoma of the esophagogastric junction. Diagn Pathol. 2014;9:125.
25. Li Z, Zou X, Xie L, Dong H, Chen Y, Liu Q, et al. Prognostic importance and therapeutic implications of PAK1, a drugable protein kinase, in gastroesophageal junction adenocarcinoma. PLoS One. 2013;8(11):e80665.
26. Chaudhary S, Kwak EL, Hwang KL, Lennerz JK, Corcoran RB, Heist RS, et al. Revisiting MET: clinical characteristics and treatment outcomes of patients with locally advanced or metastatic, MET-amplified esophagogastric cancers. Oncologist. 2020;25:e1691–700.
27. Kwak EL, Ahronian LG, Siravegna G, Mussolin B, Borger DR, Godfrey JT. Molecular heterogeneity and receptor coamplification drive resistance to targeted therapy in MET-amplified esophagogastric cancer. Cancer Discov. 2015;5(12):1271–81.
28. Gambardella V, Fleitas T, Tarazona N, Cejalvo JM, Gimeno-Valiente F, Martinez-Ciarpaglini C, et al. Towards precision oncology for HER2 blockade in gastroesophageal adenocarcinoma. Ann Oncol. 2019;30(8):1254–64.
29. Burtness B, Ilson D, Iqbal S. New directions in perioperative management of locally advanced esophagogastric cancer. Am Soc Clin Oncol Educ Book. 2014;e172–8.
30. Pellino A, Riello E, Nappo F, Brignola S, Murgioni S, Djaballah SA, et al. Targeted therapies in metastatic gastric cancer: current knowledge and future perspectives. World J Gastroenterol. 2019;25(38):5773–88.

How to cite this article: Wang ZY, Xiao W, Jiang YZ, Dong W, Zhang XW, Zhang L. HN1L promotes invasion and metastasis of the esophagogastric junction adenocarcinoma. *Thorac Cancer*. 2021;12: 650–658. https://doi.org/10.1111/1759-7714.13842